Structure of Silk Fibroin Fibers Made by an Electrospinning Process from a Silk Fibroin Aqueous Solution

Hong Wang, Huili Shao, Xuechao Hu

State Key Laboratory for Modification of Chemical Fibers and Polymer Materials, College of Material Science and Engineering, Donghua University, Shanghai 200051, People's Republic of China

Received 4 February 2005; accepted 29 November 2005
DOI 10.1002/app.24024
Published online in Wiley InterScience (www.interscience.wiley.com).

ABSTRACT: In this article, the electrospun silk fibroin (SF) fibers with an average diameter of 700 nm were prepared from a concentrated aqueous solution with an electrospinning technique. The morphology, conformation, and crystalline structure of the SF fibers were characterized by scanning electron microscopy, Raman spectroscopy, and wide-angle X-ray diffraction, respectively. The structure and morphology of the fibers were strongly influenced by the solution concentration and the processing voltage. In addition, the fiber formation parameters, including spinning velocity, elongation rate, and draw ratio, were also calculated. A kind of SF fiber with a structure between an amorphous film and a natural silk was found. We suggest that the high draw ratio was not the only factor in the transformation of SF from random-coil and α-helix conformations to a β-sheet conformation. © 2006 Wiley Periodicals, Inc. J Appl Polym Sci 101: 961–968, 2006

Key words: drawing; fibers; solution properties

INTRODUCTION

The dragline filaments produced by orb-weaving spiders have been the focus of numerous recent investigations because they are among the strongest known protein fibers.[1,2] Therefore, researchers all over the world are interested in mimicking these native silk fibers and hope to produce artificial silk fibers in vitro for industrial production.[3–5] A number of groups have attempted to spin silk protein fibers from regenerated silk or recombinant spider-silk solutions.[6–8] The solvents that have up to this point been proposed to dissolve silk fibroin (SF) may be classified into two classes:[9–12] acidic solvents (e.g., formic acid) and high-ionic-strength aqueous salt solutions. A drawback of the former solvents, which tend to be harsh and may degrade the fibroin, is the poor stability of their SF solutions. In the latter case, it is difficult to remove inorganic salts from the SF solutions. To overcome these drawbacks, Seidel et al.[13] selected hexafluoro-2-propanol (HFIP) as the solvent for the fabrication of regenerated spider-silk fibers by a wet spinning process. However, HFIP could not be removed thoroughly from the resulting fibers, and the cost was also very high. Recently, Lazaris et al.[14] prepared soluble recombinant dragline silk proteins and spun monofilaments from a concentrated aqueous solution of soluble recombinant spider-silk protein to an alcohol coagulation bath. The spun fibers exhibited toughness and modulus values comparable to those of native dragline silks but with a much lower tenacity.[14]

As with natural fibers, however, spider-silk fibers and silkworm silk fibers are spun from aqueous proteins solution to air,[15] so we are more interested in how filaments could be solidified in air from an aqueous solution. Accordingly, it was necessary to study the fiber formation mechanism of SF from an aqueous solution and to determine the factors that transform SF from random-coil and α-helix conformations to a β-sheet conformation. Furthermore, by comparison with the fiber formation conditions in the gland of the spider or silkworm, people could finally produce silk fibers from aqueous recombinant spider-silk protein solutions.

The electrospinning technique has been known since the 1930s, and interest in the electrospinning process has risen in the past decade.[16,17] Because polymer fibers prepared by this technique can have fiber diameters in the range of nanometers to a few micrometers and large specific surface areas, electrospun fibers could be used in products, such as filters, membranes, biocidal gauzes, scaffolding for tissue build-up, and even clothing, whose functions are area-

Correspondence to: H. Shao (hlshao@dhu.edu.cn).
Contract grant sponsor: Hi-Tech Research and Development Program of China (863 project); contract grant number: 2002AA336060.

based.[18] There was a preliminary report about electrospun spider-silk nanofibers with HFIP as a solvent.[19] Recently, Kim et al.[20] used formic acid as a solvent to electrospin silk nanofibers. However, all of the resultant as-spun SF fibers were only in a random-coil conformation, which was not stable enough to make the fibers into structural materials, and had to be dealt with thermal annealing or methanol treatment to increase their crystallinity.

Therefore, the objectives of this study were first to prepare a spinnable SF aqueous solution with a high SF content, second to produce ultrafine SF fibers from an aqueous solution by the environmentally friendly process of electrospinning, and third to investigate the fiber formation mechanism of the SF fibers spun from the aqueous solution.

EXPERIMENTAL

Preparation of the regenerated SF aqueous solutions

Cocoons of the *Bombyx mori* silkworm were boiled in 0.5% (w/w) $NaHCO_3$ solution for 30 min and then rinsed thoroughly with distilled water to extract the gluelike sericin proteins. Each step was repeated twice, and finally, the degummed silk was dried at room temperature. The dried degummed silk was dissolved in a 9.3*M* LiBr aqueous solution at room temperature to obtain an SF aqueous solution with a concentration of 10 wt %, which was diluted with four times the amount of water and then dialyzed against distilled water for 3 days. Then, the solution was filtered, and the final SF aqueous solutions with desired concentrations were prepared with a procedure developed in this laboratory. Through this treatment, the molecular weight of SF was between 80 and 90 kDa, as measured by sodium dodecyl sulfate-polyacrylamide gel electrophoresis (SDS-PAGE).

Electrospinning process

The SF aqueous solution was contained in a plastic syringe, which was connected to a metal needle with diameter of 0.9 mm. A flat piece of aluminum foil (the collection plate), placed 11 cm from the needle, was used to collect the electrospun product. A voltage of 10–40 kV was applied to the aluminum foil by a high-voltage power supply. The electrospinning process was carried out at room temperature, and the mass throughout was controlled by a metric pump. A schematic diagram of the electrospinning device is presented in Figure 1. The process parameters of all of the electrospun SF fiber samples of this study are summarized in Table I.

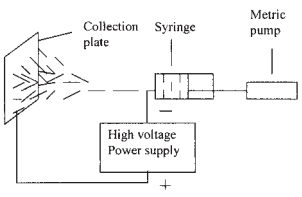

Figure 1 Schematic diagram of the electrospinning device.

TABLE I
Process Parameters of the Electrospun SF Fiber Samples

	Sample					
	L1	H1	L2	H2	L3	H3
Concentration (wt %)	17	17	28	28	39	39
Voltage (kV)	20	40	20	40	20	40

The pH value of all of these solutions was 7.68 without any addition of ions.

Measurements

The morphology of the electrospun fibers was observed with a JSM-5600LV (Jeol Co., Tokyo, Japan) scanning electron microscope at 10 kV. All samples were sputtered with gold.

Raman spectra were obtained with a Lab RAM-1B microscopy Raman microscope (HORIBA Jobin Yvon Co., Edison, NJ). The 632.8-nm red line of a He–Ne laser was focused on the samples.

Wide-angle X-ray diffraction (WAXD) patterns were measured on a Rigaku D/Max-BR diffractometer (RigaKu/MSC, the Woodlands, TX) with Cu Kα radiation (λ = 1.54 Å) in a 2θ range of 5–40° at 40 kV.

The rheological measurements were made on a RS1 Rheometer (Thermo Electron Co., Germany) with a (Ti, 35/1°) cone plate. The shear rate was linearly increased from 0.5 to 1000 s^{-1}, and the temperature was controlled at 25 ± 0.1°C.

RESULTS AND DISCUSSION

Effect of the concentration of the SF aqueous solution on the morphology of the SF fibers

Figure 2 shows the scanning electron microscopy (SEM) photographs of silk fibers prepared from SF aqueous solutions with concentrations of 17, 28, and 39 wt % (the pH value of all of these solutions was 7.68 without any addition of ions). The applied voltage was kept constant at 20 kV, and the temperature was kept at 25°C. The morphology of the SF fibers was strongly affected by the concentration of the solution. When the solution concentration was as low as 17 wt %, there were only small droplets on the aluminum foil. For the SF aqueous solution with a concentration of 28 wt %, the as-spun SF fibers exhibited a round cross-section with diameters ranging from 400 to 800 nm. However, the SF fibers prepared from the SF

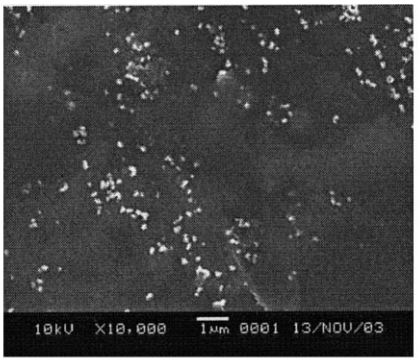

(a)

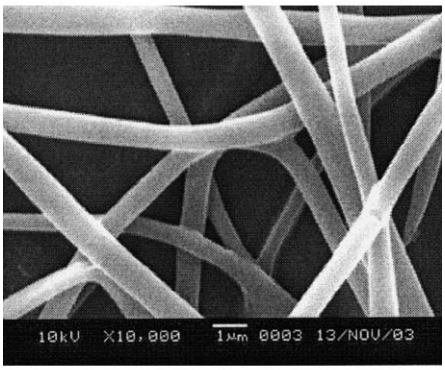

(b)

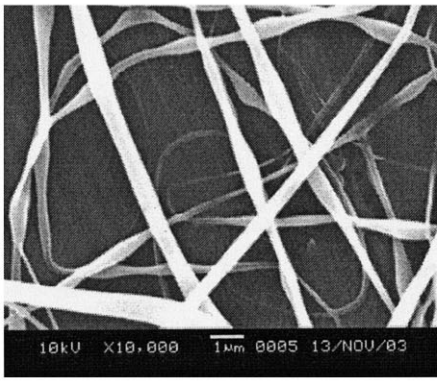

(c)

Figure 2 SEM photographs of electrospun SF fibers: samples (a) L1, (b) L2, and (c) L3.

aqueous solution with a concentration of 39 wt % became uneven and ribbon-shaped, and their diameters varied from 100 to 900 nm. In any case, all of the fibers were much thinner than natural silk fibers (*B. mori* = 10–20 μm).

It was reported[21] that sufficient molecular chain entanglements in the polymer solution can prevent the breakup of the electrically driven jet and allow the electrostatic stresses to further elongate the jet and draw it into fibers during the electrospinning process. Nevertheless, low-viscosity liquids are only deposited as individual droplets.[21]

To further investigate the influence of the solution concentration on the morphology of the electrospun SF fibers, the rheological behaviors of the SF aqueous solutions were studied. Figure 3 shows the rheological behaviors of the SF aqueous solutions with different concentrations. There was a rapid initial shear thinning at low shear rates ($\leq$10 s^{-1}) for the SF aqueous solutions with concentrations of 17 and 28 wt %; after that, their viscosities remained approximately constant. However, the shape of the rheological curve of the SF aqueous solution with a concentration of 39 wt % was different from those of the previous two SF aqueous solutions. Its viscosity was almost constant when the shear rate was lower than 1000 s^{-1}; after that, the shear thinning phenomenon became distinct.

The rheological behavior indicated that when the concentration of the SF aqueous solution was 17 wt %, the SF macromolecules might have been in a random-coil conformation with little entanglement between them. As a result, the viscosity of the solution after shear thinning was only about 40 mPa s, and the solution was deposited from the spinneret as individual droplets on the collection plate during the electrospinning process. For the SF aqueous solution with a concentration of 28 wt %, its viscosity after shear thinning reached about 250 mPa s. There might have been evidently sufficient molecular chain entanglements in the solution to prevent the breakup of the electrically driven jet and to allow the electrostatic stresses to further elongate the jet and draw it into fibers. When the concentration of the SF aqueous solution was as high as 39 wt %, the viscosity of the SF aqueous solution was sufficiently high (3000 mPa s)

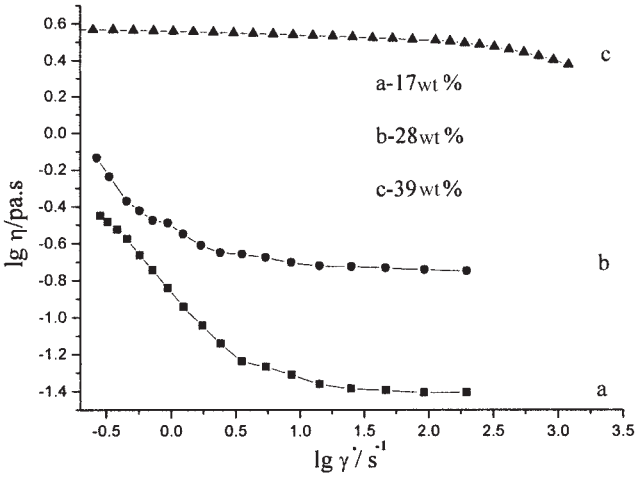

Figure 3 Rheological behaviors of SF aqueous solutions with different concentrations.

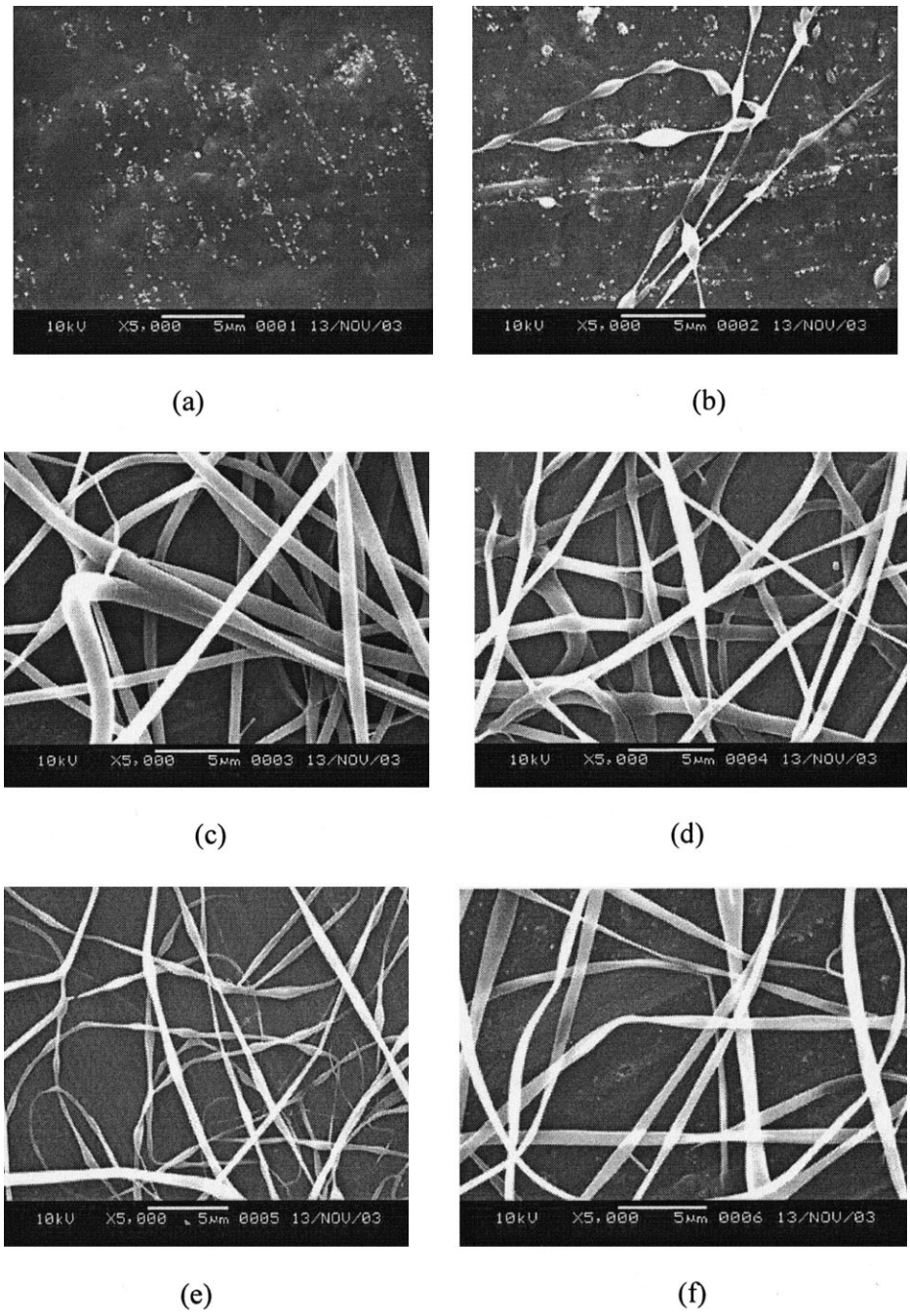

Figure 4 SEM photographs of electrospun SF fibers: samples (a) L1, (b) H1, (c) L2, (d) H2, (e) L3, and (f) H3.

that the solution could bear more tensile strain, so more thinner SF fibers appeared.

Effect of the voltage on the morphology of the SF fibers

The effect of the voltage applied during electrospinning on the SF fibers was also investigated, and the SEM photos are shown in Figure 4. For the solution with a low concentration of 17 wt %, there was little entanglement between the SF macromolecules; the polymer jet only formed droplets at low voltages because the electrostatic force could not overcome the surface tension[22] [Fig. 4(a)]. When a higher voltage was applied, the strong electrostatic force overcame the surface tension and made some random-coil SF chains more extended. However, the jet still had the tendency to contract into droplets. As a result, some beaded fibers were formed, although the viscosity of the SF solution was very low [Fig. 4(b)]. When the concentration of the SF aqueous solution was 28 wt %, the high viscosity made it form round cross-sectional

TABLE II
ν_1 Values when the SF Fibers Arrived at the Collection Plate

Concentration of the solution (wt %)	Voltage (kV)	w (g)	t_1 (min)	$r_1\times10^{-5}$ (cm)	ν_1 (m/min)
28	20	0.2247	30	6.3	4550
28	40	0.1660	29.8	5.5	4440
39	20	0.2348	30	6.8	4082
39	40	0.2154	27	6.6	4417

The density of SF fibers was set as 1.32g/cm^3, the same as that of the natural silk fiber. The spin dope was an SF aqueous solution with a pH value of 7.68 without the addition of any ions.

electrospun SF fibers with smooth surfaces at a low voltage [Fig. 4(c)]. As the intensity of the electric field was increased, the spinning rate increased quickly, so water in the jet did not have enough time to completely vaporize from the fiber surface before it arrived at the foil, and the fibers consequently became ribbonlike[23] [Fig. 4(d)]. However, when the concentration of the SF aqueous solution was as high as 39 wt %, the viscosity of the SF aqueous solution became comparatively high, which made the spinning process unstable, and fibers with irregular morphology were formed [Fig. 4(e)]. With increasing voltage, the high electrostatic power made the concentrated SF aqueous solution flow more easily, so the resultant fibers became more regular in comparison with sample L3 [Fig. 4(f)]. For the same reason, the viscosity of the 39 wt % SF aqueous solution was comparatively high; it was not easy for water in the jet to diffuse and vaporize from the fibers surface before they arrived at the collection plate, and the SF fibers became ribbonlike again.

In conclusion, the solution concentration and spinning voltage had some influence on the morphology of the SF fibers. The electrospinning conditions for the production of beadless round silk fibers from the SF aqueous solutions were found to be as follows: SF concentration = 28 wt %, voltage = 20 kV, and working distance = 11 cm.

Calculation of the SF fiber formation parameters

To get a better understanding of the SF fiber formation during electrospinning and the conformation transition of SF, the fiber formation parameters in these experiments were calculated.

Spinning velocity (ν_1) of the SF fiber when it arrived at the collection plate

Fang and Reneker[24] studied the electrospinning process systematically. They pointed out that a single jet did not break up during fiber formation; this concept is well accepted.[25,26] On the basis of this assumption and with the supposition that the water in the fiber evaporated completely, ν_1 of SF fibers when they arrive at the collection plate can be calculated by the following equation:

$$\nu_1 = \frac{w_1}{100\rho_1\pi r_1^2 t_1} \quad (1)$$

where ν_1 is the spinning velocity when the fibers arrive at the collection plate (m/min), w_1 is the weight of the fibers on the collection plate (g) during a certain spinning time, ρ_1 is the density of the fibers (g/cm^3), r_1 is the radius of the fibers (cm), and t_1 is the spinning time (min).

The applied voltages were set as 20 and 40 kV, and the concentration of the solutions were 28 and 39 wt %, respectively. The results of the calculations are shown in Table II.

As shown in Table II, ν_1 was about 4000–4500 m/min, which was already in the high-speed spinning range. We guessed that the fibers might have experienced a strong extension in the electric field.

Ejecting velocity (ν_2) of the SF aqueous solution from the spinneret

During the electrospinning process, the SF aqueous solution experienced a shear flow; then, it was ejected from the spinneret and drawn by electrostatic force to finally form fibers. To get the draw ratio (λ), it was necessary to calculate ν_2 of the SF aqueous solution when it left the spinneret. According to the principle of mass conservation and by the measurement of the weight of the SF aqueous solution in a certain time (w_2) during the electrospinning process, ν_2 of the SF aqueous solution when it left the spinneret was obtained as the following equation:

$$\nu_2 = \frac{w_2}{100\rho_2\pi r_2^2 t_2} \quad (2)$$

where ρ_2 is the density of the SF aqueous solution (g/cm^3), r_2 is the diameter of the spinneret (cm), and t_2

TABLE III
ν_2 Values of the Solutions when They Left the Spinneret

Concentration of the solution (wt %)	Voltage (kV)	w_2 (g)	t_2 (min)	$\nu_2 \times 10^2$ (m/min)
28	20	0.6299	30	3.1
28	40	0.4539	29.8	2.2
39	20	0.8040	30	3.8
39	40	0.5952	27	3.1

The densities of water and the natural silk fiber were 1.0 and 1.32g/cm^3, respectively, so the density of the SF aqueous solutions with concentrations of 28 and 39 wt % were set as 1.07 and 1.12 g/cm^3, respectively, according to the law of constant proportion. The spin dope was an SF aqueous solution with a pH value of 7.68 without the addition of any ions.

is the spinning time (min). Here, r_2 can be measured by a special microscope.

The applied voltages were set as 20 and 40 kV, and the concentrations of the SF aqueous solutions were 28 and 39 wt % (the pH value of all of these solutions was 7.68 without any addition of ions), respectively. The results of the calculation are shown in Table III. The SF aqueous solution passed through the spinneret very slowly at a rate of about 3×10^{-2} m/min.

Elongation rate (ε) and λ of the SF fiber

It is well known that ε of the fiber can be written as follows:[27]

$$\varepsilon = d\nu/dl \approx \Delta\nu/\Delta l \quad (3)$$

where $d\nu$ is the velocity of the running filament, dl is the distance from the spinneret along the spinning path, $\Delta\nu$ is the difference between the spinning velocity and the ejecting velocity, and Δl is the difference between the spinneret and the collection plate.

Similarly, λ can be written as follows:[27]

$$\lambda = \nu_1/\nu_2 \quad (4)$$

where ν_1 and ν_2 are the spinning and ejecting velocities, respectively. The results are shown in Table IV.

As shown in Table IV, ε and λ of the SF fiber during electrospinning were very high. ε reached orders of 10^2, and λ reached orders of 10^5, which are very difficult to achieve in a common spinning process. To make a comparison, λ of the SF aqueous solution in the gland of silkworm when a silkworm spins silk at an average rate of 1 cm/s[28] was also calculated. λ was about 1.33×10^4, which was close but still lower than that of the SF aqueous solution during the electrospinning process. Therefore, we suggest that the SF macromolecular chains were extended at such a high λ in the electric field that some SF chains transferred to β-sheet conformations and finally precipitated from aqueous solution to form SF fibers. The following measurements showed that some changes in the conformation and crystallization of the SF molecular did happen, but they were still quite different from the conformation and crystalline structure of natural silk. This implied that a high λ was not enough to transfer the random-coil or α-helix conformation to a β-sheet structure. To get a β-sheet structure, other conditions need to be considered.

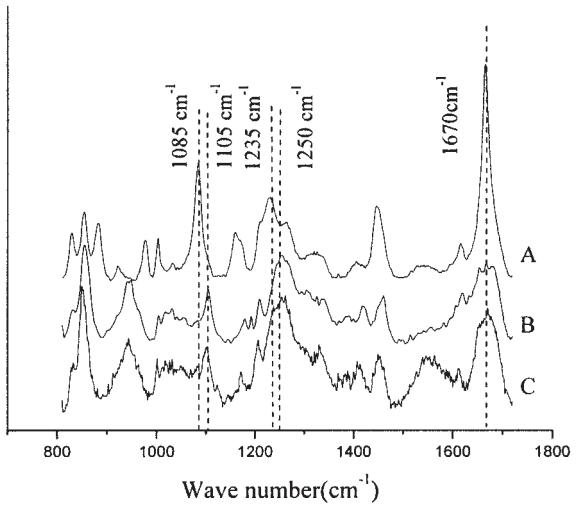

Figure 5 Raman spectra of the (A) degummed silk fibers, (B) amorphous SF film, and (C) electrospun SF fibers.

Secondary structure of the electrospun SF fibers

Raman spectroscopy is a powerful tool for investigating the secondary structure of proteins, and it has already given important insights into the structure of

TABLE IV
ε and λ Values During the Electrospinning Process

Concentration of the solution (wt %)	Voltage (kV)	ν_1 (m/min)	$\nu_2 \times 10^{-2}$ (m/min)	ε (s^{-1})	$\lambda \times 10^5$
28	20	4550	3.1	690	1.47
28	40	4440	2.2	672	2.02
39	20	4082	3.8	730	1.07
39	40	4417	3.1	670	1.42

native silk filaments of both spiders and silkworms.[29,30] Figure 5 shows the Raman spectra of the degummed silk fibers, amorphous SF film, and electrospun SF fibers obtained from the SF aqueous solution with a concentration of 39 wt % at a voltage of 40 kV.

All of the secondary structures of proteins (α-helix, β-sheet, and random-coil) have characteristic bands at amide I (1680–1640 cm^{-1}) and amide III (1270–1220 cm^{-1}).[31] Their characteristic bands in the Raman spectrum are as follows: 1250 and 1660 cm^{-1} (random-coil), 1270 and 1655 cm^{-1} (α-helix), and 1235 and 1670 cm^{-1} (β-sheet). Moreover, the peaks at 1105 and 1085 cm^{-1} are sensitive to α-helix and β-sheet conformations, respectively. As a benchmark and shown in Figure 5, the amide I and amide III bands of the degummed silk fibers appeared at about 1670 and 1230 cm^{-1}, and the peak at 1085 cm^{-1} was also obvious, which suggested that the degummed silk fibers were in the β-sheet structure. The amide III band of the amorphous SF film appeared at 1250 cm^{-1} and was associated with the random-coil conformation; the peak at 1105 cm^{-1} indicated that it also had an α-helix conformation. Compared to the amorphous SF film, the amide I band of the electrospun SF fibers was sharper at 1670 cm^{-1}, the amide III band split into 1230 and 1250 cm^{-1}, and the peak at 1085 cm^{-1} was enhanced, which suggested they had a certain amount of β-sheet conformation.

Crystal structure of the electrospun SF fibers

It was reported that SF exhibits at least three conformations or crystalline structures: random coil, silk I, and silk II. Silk II is commonly thought to be constituted by β sheets.[32] A number of models for silk I have been proposed.[33,34] The popular crankshaft model proposes antiparallel hydrogen bonded sheets wherein alternating alanyl and glycyl units are in β-sheet conformations and left-handed α-helix conformations, respectively. Silk II is the most stable structure, and it endows silk fibers with excellent mechanical properties. By WAXD measurement, some information about the crystalline structure of the SF fibers were obtained from their crystal structure transitions. The principal X-ray diffraction peaks of silk II appeared at 9.7×10^{-10} m ($2\theta = 9.1°$), 4.69×10^{-10} m ($2\theta = 18.6°$), 4.3×10^{-10} m ($2\theta = 20.7°$), and 3.67×10^{-10} m ($2\theta = 24.3°$).[35] Figure 6 shows the WAXD patterns of the degummed silk fibers, amorphous SF film, and electrospun SF fibers obtained from the SF aqueous solution with a concentration of 39 wt % at a voltage of 40 kV. The amorphous SF film showed an amorphous state, whereas the degummed silk fibers exhibited a typical X-ray diffractogram of a β-sheet crystalline structure, which had three diffraction peaks at 18.9, 20.6, and 28.1°, corresponding to β-sheet crystalline spacings of 4.69, 4.31, and 3.66 Å, respectively. There were diffraction peaks at $2\theta = 14.5$ and 17.6° in the electrospun SF fibers, which was different from the silk II crystal structure and which means that the SF macromolecules underwent a conformation transition during the electrospinning process. The crystalline structure appeared in the electrospun SF fibers, but it was not like the crystal structure we found in natural silk.

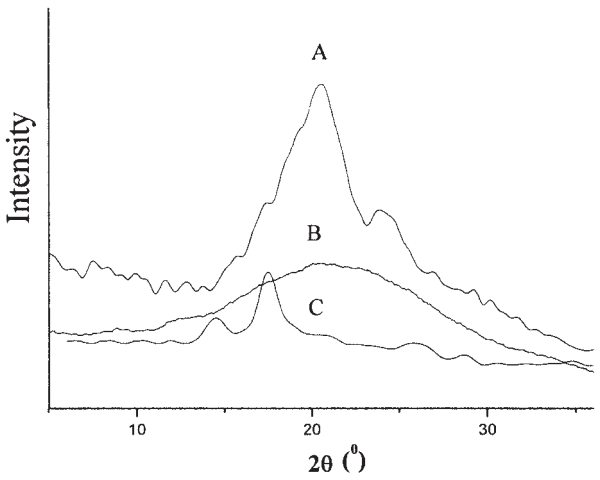

Figure 6 WAXD patterns of the (A) degummed silk fibers, (B) amorphous SF film, and (C) electrospun SF fibers.

CONCLUSIONS

In this study, beaded, cylinder-shaped and ribbon-shaped ultrafine elecrospun SF fibers were obtained from concentrated aqueous solutions under different conditions with the electrospinning technique. These fibers had an average diameter of 700 nm ranging from 100 to 900 nm. The morphology of the SF fibers was strongly influenced by the solution concentration and the processing voltage. The conditions for the preparation of beadless round electrospun SF fibers were found to be as follows: concentration = 28 wt %, voltage = 20 kV, and working distance = 11 cm.

From the investigation of Raman spectroscopy and WAXD, we found that there was some β-sheet conformation and crystalline structure in the electrospun SF fibers, but they were still different from the structure we found in natural silk. Through the calculation of the fiber formation parameters, such as ν_1, ε, and λ, we found that even with very high λ random-coil conformation and α-helix structure could not fully transfer to β-sheet forms like those of spider or silkworm silk.

References

1. Knight, D. P.; Shao, Z. Nature 2000, 418, 741.
2. Viney, C. J Text Inst 2000, 3, 2.

3. Chen, X.; Shao, Z.; Knight, D. P.; Vollrath, F. Acta Chim Sinica 2002, l60, 2203.
4. Hyoung-Joon, J.; Kaplin, D. L. Nature 2003, 428, 1057.
5. Rieket, C.; Vollrath, F. Int J Biol Macromol 2001, 29, 203.
6. Chen, X.; Knight, D. P.; Shao, Z.; Vollrath, F. Biochem 2002, 141, 14944.
7. Shao, Z.; Vollrath, F.; Yang, Y.; Thogersen, H. C. Macromolecules 2003, 36, 1157.
8. Arcidiacono, S.; Mello, C. M.; Michelle, B.; Elizabeth, W.; Spares, J. W.; Alfred, A.; David, Z.; Thomas, L.; Suasan, C. Macromolecules 2002, 35, 1262.
9. Gustavus, J.; Esselen, S. U.S. Pat. 1,934,413 (1933).
10. Camille, D.; George, W. M. U.S. Pat. 1,936,753 (1933).
11. Jpn. Pat. 2002363861.
12. Ishizaka, H.; Watanabe, Y.; Ishida, K. J Seric Jpn 1989, 58, 87.
13. Seidel, A.; Liivak, O.; Jelinski, L. W. Macromolecules 1998, 31, 6733.
14. Lazaris, A.; Arcidiacono, S.; Huang, Y.; Zhou, J. F.; Duguay, F.; Chretien, N.; Welsh, E. A.; Soares, J. W.; Karatzas, C. N. Science 2002, 295, 472.
15. Iizuka, E. J Polym Sci Polym Symp 1985, 41, 163.
16. Zeng, J.; Chen, X. S.; Xue, X. Y. J Appl Polym Sci 2003, 89, 1085.
17. Krishnappa, R. V. N.; Desai, K.; Sung, C. M. J Mater Sci 2003, 38, 2375.
18. Zhong, X. H.; Ran, S. F.; Fang, D. F. Polymer 2003, 44, 4959.
19. Zarkoob, S.; Reneker, D. H.; Eby, R. K. Polym Prepr 1998, 39, 244.
20. Kim, S. H.; Nam, Y. S.; Lee, T. S.; Park, W. H. Polym J 2003, 35, 185.
21. Fong, H.; Chun, I.; Reneker, D. H. Polymer 1999, 40, 4585.
22. Son, W. K.; Youk, J. H.; Lee, T. S.; Park, W. H. Polymer 2004, 45, 2959.
23. Frenot, A.; Ioannis, S. C. Curr Opin Colloid Ind 2003, 8, 64.
24. Fang, X.; Reneker, D. H. J Macromol Sci Phys 1997, 36, 169.
25. Doshi, J.; Reneker, D. H. J Electrost 1995, 35, 151.
26. Hohman, M.; Shin, M.; Rutledge, G. C.; Brenner, M. P. Phys Fluids 2001, 13, 2201.
27. Ziabicki, A. Fundamentals of Fiber Formation: The Science of Fiber Spinning and Drawing; Wiley: New York, 1976.
28. Magoshi, J.; Magoshi, Y.; Nakamura, S. J Polym Sci Polym Symp 1985, 41, 187.
29. Zheng, S.; Li, G.; Yao, W.; Yu, T. Appl Spectrosc 1989, 43, 1269.
30. Shao, Z.; Vollrath, F.; Sirichaisit, J.; Young, R. J. Polymer 1999, 40, 2493.
31. Ming-Zhong, L.; Zheng-Yu, W.; Minoura, N.; Hao-Jing, Y. J Donghua Univ (Eng Ed) 2002, 19, 1.
32. Marsh, R. E.; Corey, R. B.; Pauling, L. Biochem Biophys Acta 1975, 16, 1.
33. Lotz, B.; Keith, H. D. J Mol Biol 1971, 61, 201.
34. Ishikawa, H.; Nagura, M. Sen-i Cakkaishi 1983, 39, 353.
35. Asakura, T.; Kuzuhara, A.; Tabeta, R.; Saito, H. Macromolecules 1984, 18, 1841.